Materials Science in Semiconductor Processing 33 (2015) 49–57

Contents lists available at ScienceDirect

Materials Science in Semiconductor Processing

journal homepage: www.elsevier.com/locate/mssp

Kinetics of light-induced degradation in compensated boron-doped silicon investigated using photoluminescence and numerical simulation

K. Fraser [a,*], D. Blanc-Pelissier [a], S. Dubois [b], J. Veirman [b], M. Lemiti [a]

[a] Institut des Nanotechnologies de Lyon (INL), UMR 5270, University of Lyon, INSA-Lyon, 20 rue Albert Einstein, 69621 Villeurbanne Cedex, France

[b] CEA, LITEN, INES, 50 av. du Lac Léman, F-73377 Le Bourget du Lac, France

ARTICLE INFO

Available online 11 February 2015

Keywords:
Photovoltaics
Silicon
Light-induced degradation
Photoluminescence
Modeling

ABSTRACT

We use photoluminescence to observe light-induced degradation in silicon in real time. Numerical simulations are used to match our results and lifetime decay data from the literature with theoretical models for the generation of the light-induced boron–oxygen defects. It is found that the existing model of the slowly generated defect SRC, where its saturated concentration is a function of the majority carrier concentration, does not explain certain results in both p- and n-type samples. A new model is proposed in which the saturated SRC concentration is controlled by the total hole concentration under illumination.

1. Introduction

Light-induced degradation (LID) in silicon (Si) containing boron (B) and oxygen (O) has been documented and investigated extensively in the literature as it is known to reduce the efficiency of solar cells made of Czochralski silicon (Cz-Si). The phenomenon was originally studied in p-type Si doped only with B [1–5], and it was found that the maximum normalized defect concentration ($N_t^*=(1/\tau)-(1/\tau_0)$, where τ_0 and τ are the minority carrier lifetime values before and after complete degradation) was proportional to the total B concentration and the square of the interstitial O (O_i) concentration. The defect generation rate was found to be proportional to the square of the equilibrium hole concentration p_0. Subsequent work [6,7] on compensated p-type Si co-doped with boron and phosphorus (P) found that N_t^* was proportional to $p_0[O_i]^2$ in such material (where p_0 cannot be assumed to be equal to $[B]$). Separate work [8] on compensated n-type Si, however, found that the maximum defect concentration did not vary with doping.

Due to the relationship between N_t^* and $[O_i]^2$, the oxygen dimer O_{i2} is assumed to be involved in the formation of LID defects. Two separate BO_{i2} defects have been identified in p-type Si by evaluating N_t^* as a function of time [5]: a fast-generated one (FRC) and a slow-generated one (SRC). SRC is often assumed not to appear in n-type Si over the timescales normally used, due to the slower generation rate in n-type Si at low excitation. The precise nature of both defects is still unknown; however, the activation energies for their generation and some of their other properties (in particular their recombination parameters) have been measured [7]. FRC is suggested to be formed by a substitutional boron (B_s) atom and SRC by an interstitial boron atom (B_i).

The kinetics of LID has generally been observed by measuring effective carrier lifetime using photoconductance techniques before and after illumination for various time intervals. In this work, we investigate LID in compensated p- and n-type Si by using photoluminescence (PL) to observe minority carrier lifetime decay in real time. We also use

* Corresponding author.
E-mail address: keithjf82@gmail.com (K. Fraser).

http://dx.doi.org/10.1016/j.mssp.2015.01.016
1369-8001/

numerical simulations to relate new and existing models of the parameters governing LID to both our own PL results and lifetime decay data from the literature.

Table 1 gives definitions of symbols used in formulae in this paper as an aid to the reader.

2. Material and methods

2.1. Samples

Samples were prepared from a Czochralski-grown silicon (Cz-Si) ingot heavily doped with both B and P. The dopant concentrations were measured via a combination of glow discharge mass spectrometry, inductively coupled plasma mass spectrometry and Hall effect measurements [10]. Fig. 1 shows how the doping varies along the length of the ingot; $[B]$ varies from ~ 2.8 to $4.4\times10^{17}\,\text{cm}^{-3}$ in the samples examined, while $[P]$ varies from ~ 1.6 to $6.7\times10^{17}\,\text{cm}^{-3}$. The resulting values are consistent with the Scheil equation [11] given segregation coefficient values of 0.8 for B and 0.35 for P. The $[O_i]$ values measured using Fourier transform infrared (FTIR) analysis, which are of the order of 10^{18}cm^{-3}, are shown on the same axes, as are values of majority carrier concentration. To calculate C_{maj} accurately, the Fermi level was computed for each sample by balancing the total charge density (Eq. (1)) [12]. This takes incomplete ionization of the dopants into account. The material is p-type (i.e. the majority carriers are holes) when the ingot fraction F is below ~ 0.7, where $[B]>[P]$; beyond this point, $[P]>[B]$ and the material becomes n-type (with electrons as majority carriers).

$$n_i \exp\left(\frac{E_I-E_F}{kT}\right)-n_i\exp\left(\frac{E_F-E_I}{kT}\right)-[B]\left(1+4\exp\left(\frac{E_B-E_F}{kT}\right)\right)^{-1}+[P]\left(1-\left(1+2\exp\left(\frac{E_P-E_F}{kT}\right)\right)^{-1}\right)=0 \quad (1)$$

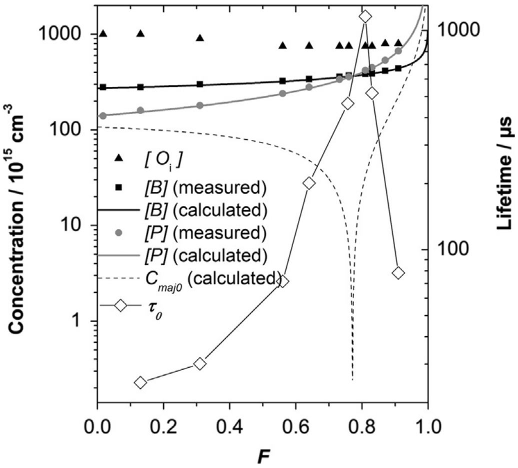

Fig. 1. Values of doping, oxygen and majority carrier concentrations and minority carrier lifetime (measured at $\Delta C=3\times10^{15}\,\text{cm}^{-3}$) along the length of the ingot from which samples used for photoluminescence experiments were prepared. See Table 1 for symbol definitions.

Table 1
Summary of symbols used in text.

Symbol	Definition
F	Fractional distance along ingot (0=first solidified Section, 1=final solidified section)
t	Elapsed time in s
r	Radial distance from centre of PL illumination spot in cm
z	Vertical distance from sample front surface in cm
E_F	Fermi energy in J
E_I	Mid-band energy level (half-bandgap width) in J
E_B,E_P	B and P energy levels in Si bandgap (relative to valence band energy) in J
n_i	Intrinsic carrier concentration in cm^{-3}
p, n	Total concentration of holes/electrons in cm^{-3}
p_0, n_0	Equilibrium (zero-excitation) concentration of holes/electrons in cm^{-3}
ΔC	Excess carrier concentration in cm^{-3}
C_{maj0}	Equilibrium majority carrier concentration in cm^{-3}
C_{min}	Total minority carrier concentration in cm^{-3}
$[B]$, $[P]$, $[O_i]$	Concentration of B/P/interstitial O in cm^{-3}
r_C	Compensation ratio of silicon doped with B and P
R	Total electron–hole pair recombination rate in $\text{cm}^{-3}\,\text{s}^{-1}$
B_{bb}	Band-to-band recombination coefficient, equal to $4.73\times10^{-15}\,\text{cm}^{-3}\,\text{s}^{-1}$ at 300 K [9]
τ, τ_0	Minority carrier lifetime in s (general and pre-degradation)
N_t	Normalized boron–oxygen defect density in s^{-1}
μ	Carrier mobility in $\text{cm}^2\,\text{V}^{-1}\,\text{s}^{-1}$
D	Ambipolar carrier diffusion coefficient in $\text{cm}^2\,\text{s}^{-1}$
I	Laser power density in W cm^{-2}
E_{ph}	Photon energy in J
α	Optical absorption coefficient in cm^{-1}
G	Optical electron–hole pair generation rate in $\text{cm}^{-3}\,\text{s}^{-1}$
S_{PL}	Photoluminescence signal (units vary)
$g_{FRC,SRC}$	Coefficients in s^{-1} controlling dependence of FRC/SRC generation rate on p
$A_{FRC,SRC}$	Activity of FRC/SRC defect in s^{-1}
$A_{SAT(FRC,SRC)}$	Maximum activity of FRC/SRC defect in s^{-1}
A_1, A_2, A_{3a}, A_{3b}, A_4	Coefficients controlling variation of A_{SAT} values with different parameters